AADE-06-DF-HO-21

Predicting Mud-Removal Efficiency During Completion-Fluid Displacements

Mario Zamora, William Foxenberg, and Sanjit Roy, M-I SWACO

Abstract

A new process has been developed to predict cleaning efficiency during mud-to-completion-brine displacements. It involves simple laboratory tests to determine the effectiveness and compatibility of wash chemicals, and an empirical model that uses these data to critically evaluate complex chemical and hydrodynamic effects under transient conditions. The process is being used for design and evaluation of displacement spacer trains with the ultimate goal of complete removal of residual mud from downhole tubulars. Modeling is especially valuable for clean-up of synthetic-based mud, which can be particularly difficult to effectively remove from pipe surfaces because of the base fluid's natural affinity for steel.

The primary purpose of this paper is to describe and discuss various elements of this analytical process, including the test procedure, the transient cleaning model, and the advanced software used for analysis. Case histories also are presented to illustrate its use.

Introduction

There was a time when procedures for displacing oil-based mud (OBM) and synthetic-based mud (SBM) with clear brine were designed with rules-of-thumb based primarily on experience. In many cases, these procedures provided a wellbore clean enough to accept a clear-brine completion fluid and continue the completion process with minimal additional clean-up steps. However, as well profiles became more complicated and displacements more challenging, procedures based on traditional guidelines sometimes produced less-than-satisfactory displacements.

As a result, various sophisticated software systems were developed to supplement experience-based design tools.[1] Until recently, however, most of these programs provided displacement guidelines that dealt primarily with volumes, pressures, and hydraulics. The spacers that separate the mud from completion fluid and perform the cleaning function of the wellbore were left to traditional design rules. Volumes and chemistry of the cleaning spacers were qualified primarily on their ability to satisfy requirements placed on the design by the system hydraulics.

Recent software enhancements now facilitate engineered displacement designs incorporating optimum spacer chemistries, volumes, and sequences to achieve a clean wellbore after a single pass of the spacer train. This software is being used as a displacement design tool to predict the effectiveness of the spacer train in entrapping and cleaning non-aqueous drilling fluids from downhole tubular surfaces. Synthetic-based mud can be particularly difficult to effectively remove from pipe surfaces because of the base fluid's natural affinity for steel.

The technology is based on a transient analysis technique developed specifically to predict mud-removal efficiency during mud-to-brine displacements. Starting point for the empirical model development was a laboratory study undertaken to determine the cleaning efficiency of a proven displacement surfactant as a function of flow-rate, surfactant concentration, contact time, and mud contamination. Results from additional laboratory flow-loop studies also were incorporated to empirically simulate fluid-fluid interfaces during the displacement.

The key elements of this transient process are the primary subjects of this paper. The transformation of data from simple laboratory tests into a format useable by the model is of particular interest. The tests normally are run using the specific fluids that will be involved in the displacement. Also discussed are the software design tool that integrates and processes this technology and several case histories that illustrate its use.

Displacement Design Considerations

A good mud-to-brine displacement is the first and arguably the most important process of a successful completion. Efficient and complete removal of residual mud from the wellbore is paramount to affect proper function of downhole tools and to reduce the risk of damage to the completion. Poorly designed or executed displacements can lead to expensive rig delays, workovers, or in the extreme case, failed completions. Permeability of gravel packs contaminated by residual mud can be significantly reduced. Gravel-pack completions also require tools to function within tight tolerances that easily can be restricted by solids.

Optimum design for many mud-to-brine displacements is often constrained by rig-pump horsepower or differential pressure limitations in the wellbore imposed by liner tops, squeezed perforations,

open-hole configurations, etc. High flow rates, viscous spacers, and wide density differentials can produce excessive pressures in the wellbore and/or at the surface. Such circumstances can make it difficult to design efficient cleaning spacers, which typically work best when formulated in fresh water and pumped at high flow rates.

Beyond these pressure and hydraulics issues, engineered spacer-train design also must address effectiveness (chemistry), contamination (interfaces), contact time (volume), and flow regime (flow rate, geometry, viscosity). Determining how different combinations might affect mud-removal efficiency can be challenging even if case-history information is available.

Unfortunately, there are no currently available direct or indirect means to measure whole mud or mud film remaining downhole during and after the displacement process. Instead, mud-to-brine displacement quality is commonly inferred from indicators such as brine turbidity, filtration-cycle requirements, and interface volumes. Labor-intensive laboratory analyses of flow-back samples collected at critical stages of the displacement also have been used to evaluate and displacement quality.[1]

Computer simulation to assist with the design of mud-to-brine displacements would seem a viable option; however, prediction of mud-removal efficiency is a complex task involving a number of dynamic processes and parameters. Development of a new empirical model to handle this task is described next. The computer software that addresses the combined displacement concerns is discussed in a separate section.

Model for Mud-Removal Prediction

Because of complexities associated with the displacement process, development of purely analytical models simply was not feasible. Instead, it was decided to focus on empirical relationships based on laboratory testing to quantify the effectiveness and compatibility of the wash chemicals being considered for the well-specific displacement. The model would have to use these data to critically evaluate physical, chemical, and hydrodynamic effects under transient conditions. Analyses would further be complicated by multiple fluid-fluid interfaces that develop downhole during the displacement and systematically contaminate the spacer pills. Since interfaces are complicated in their own right, additional laboratory studies were commissioned to establish empirical relationships that also could be incorporated into the final software analyses.

The major modeling challenge was to develop a practical method to integrate the targeted laboratory results into the process. The basic displacement models involving hydraulics, pressures, and volumes had been implemented successfully in earlier versions[6] of the software that now has been upgraded to include prediction of mud-removal efficiency. The same finite-difference method proved to be quite suitable for handling transient behavior for the application at hand.

Laboratory Cleaning Study

Currently, there are no industry-standard or API-recommended laboratory methods for evaluating the effectiveness of solvents, surfactants, and dispersants used for well cleaning. With notable variations, however, tests based around standard oilfield rotational viscometers have been used for some time.[2,3,4,5] Controlled mixing by the ubiquitous viscometer creates dynamic environments simulating flow past tubulars.

In most versions of this type of test, the rotor is replaced with a carbon-steel or sand-coated sleeve to provide a more realistic surface for mud to adhere. The rotor speed sometimes is set at 100 or 200 rpm to roughly approximate expected shear rates. Visual inspection and weight of the mud-coated rotor are the most common techniques used to estimate the mud film remaining on the rotor (or “degree of cleanliness”) after selected stages in the test procedure.

The laboratory study used to develop the overall model was designed to investigate mud-film removal for the combined effects of velocity, surfactant concentration, surfactant-solution contamination, and contact time. Tests were run on a 12-speed rotational viscometer fitted with a 1.575-in OD carbon-steel rotor (no bob). An API thermocup was used to maintain test fluids at 150°F. The drilling fluid was an 11.1-lb/gal synthetic-based field mud obtained from a deepwater, Gulf of Mexico project. A detergent/surfactant designed for oil and synthetic-based muds was mixed in seawater to formulate the wash spacer.

The sleeve was first coated with mud while rotating at 6 rpm for 5 min to start each test series. The coated sleeve was then rotated at different test speeds in wash pills contaminated by the drilling fluid. Cleaning efficiency was determined by visual inspection at the end of each preset contact-time interval. Efficiency was qualitatively assigned a rating from 1 to 5 (1 for 100% cleaning and 5 for no perceptible cleaning).

The tests were structured to permit statistical analysis of the results to simulate transient behavior. Specific test parameters included the following:

- Viscometer speeds of 600, 300, 100, 60, 6, and 0.9 rpm
- Surfactant concentrations of 0, 5, 10, and 25% v/v
- Spacers contaminated with mud at 0, 25, 50, and 75% v/v levels
- Cumulative contact times of 0.5, 1.5, 3.7, 5 and 10 min (for each combination of speed, surfactant concentration, and contamination level).

Goal of the study was to create a full data matrix among all the parameters in order to permit use of interpolation techniques for the transient analyses. A

small sample of the laboratory test results is presented in **Table 1** as a function of rotor speed (rpm), surfactant concentration (% v/v), and contamination level (% v/v). Blank cells in **Table 1** indicate test conditions where data were not taken because of time constraints. The study included 31 test series out of the 96 possible (6 viscometer speeds x 4 surfactant concentrations x 4 contamination levels).

The visual inspection method worked quite well, the quality of which was later confirmed by data analysis. All test results were run and evaluated by the same research engineer in a uniform and systematic manner. (Since then, weight measurements have been added to the test procedure to support observations.) In order to simplify the analysis, the ratings were converted to Cleaning Indexes expressed as decimal values, where 1.0 represented a completely clean rotor. These are listed for each test series under the different time intervals in **Table 1.**

Modeling using Type Curves

Initial attempts to use conventional evaluation techniques to complete the full matrix were unsuccessful. Instead, it was decided to use type curves to characterize and extrapolate the measured data. Sigmoid functions were selected because they fit the data trends when plotting cleaning efficiency vs time and seemed to be in sync with the physical process.

Parallels between sigmoid curves and wellbore cleaning are evident from the data set. For much of the data, mud removal by the flowing fluid started slowly, increased then decreased exponentially, and eventually reached a steady state, maximum level. Clearly, cases involving high rotor speeds and/or surfactant concentrations provided different results than cases for which the wash fluid was contaminated, the rotor speeds were low, and the surfactant concentration was minimal.

Sigmoid curves can be defined mathematically in a number of ways. The simplest, most recognizable form is given below:

$$CI(t) = 0 \quad \text{for } t \le 0 \qquad \text{Eq. 1a}$$
$$= 2t^2 \quad \text{for } 0 \le t \le \beta \qquad \text{Eq. 1b}$$
$$= 1 - 2(1-t)^2 \quad \text{for } \beta \le t \le 1 \qquad \text{Eq. 1c}$$
$$= 1 \quad \text{for } t \ge 1 \qquad \text{Eq. 1d}$$

$$\text{where } \beta = 0.5 \quad \text{crossover} \qquad \text{Eq. 1e}$$

The value for Cleaning Index "CI" is a function of the independent variable contact time "t". As seen above, the sigmoid curve for CI is a composite consisting of mirror images, with one equation for t values below the crossover point β and another for t values above β.

A generalized form of the sigmoid curve was derived for use as a powerful curve-fitting tool to characterize the experimental data set. The crossover point β was redefined as a function of two parameters that are used to establish two different sets of type curves. The "Max" type curves relate to the maximum cleaning that can be achieved in a time-based test series. The "Level" type curves are used for predefined rates at which cleaning occurs vs contact time. Both type curves are used in combination to define the complete data set.

Cleaning Index vs Normalized Contact Time type curves are plotted in **Figs. 1a-1d** and **Figs. 2a-2f** at four discrete "Max" values and six discrete "Level" values. The same data points (as open circles and squares) are used in all of these graphs. They represent a matrix of all practical combinations that could be derived from the experimental data, assuming that the visual inspection values are limited to integer values and the time intervals match the testing specifications.

A generalized sigmoid curve version presented below was derived to accept Max and Level response values.

$$CI = 0.5\, m\, (t / \beta)^{e1} \quad \text{for } t \le \beta \qquad \text{Eq. 2a}$$
$$CI = m - 0.5\, m\, [(1 - t)/(1 - \beta)]^{e2} \quad \text{for } t \ge \beta \qquad \text{Eq. 2b}$$

$\beta = f(m, v)$	crossover	Eq. 2c
$e_1 = f(m, \beta)$	exponent for $t \le \beta$	Eq. 2d
$e_2 = f(v)$	exponent for $t \ge \beta$	Eq. 2e
$v = 0$ to 5	level response curve	Eq. 2f
$m = 0$ to 1	maximum cleaning value	Eq. 2g
$t = 0$ to 1	normalized contact time	Eq. 2h

Continuous functions were developed for β, e_1, and e_2 based on the data set. It was experimentally determined that β was a function of m and v, e_1 was a function of m and β**,** and e_2 depended only on v.

Individual values for m and v were selected to precisely define and characterize each test series within the framework of the type curves. This was accomplished by manual, systematic curve fits that respected the position of each test series in the experimental data set. These values have been added to the **Table 1** partial data set and presented as **Table 2**. The original test-matrix data are in black; synthesized data are shown in blue.

The two time-based parameters in **Table 2** are used to characterize the data set. "Max" (0 -1) refers to the maximum cleaning index for a given test series. "Level" (0 – 5) identifies the type curve indicating the cleaning performance (initial cleaning rate and time to reach the maximum expected value, with "5" signifying the fastest overall rate). Max and Level are real-number designations (0-1 and 0-5, respectively) that characterize individual test series. This implies that a two-dimensional spectrum of type curves can be generated as functions of Max and Level.

In addition, the type curves add a synthetic (but realistic) level of precision to the data set. Consider, for example, two distinct tests that have identical maximum

cleaning indexes of 0.5. The results would be well within the precision of the visual inspection technique, despite the fact that one test should have yielded a higher efficiency. Application of type-curve analysis could adjust the respective Max values to 0.45 and 0.55, more in line with expected results. The methods used to extrapolate and construct the family of type curves are discussed later in this document.

Example model predictions vs normalized contact time using the type curves are shown in **Figs. 3a-3d** for surfactant concentrations of 5% and mud contamination levels of 0, 25, 50, and 75%. For comparison, **Figs. 4a-4c** illustrate results at 50% contamination for 0 (seawater), 10 and 25% surfactant concentrations.

The curves in **Figs. 3** and **4** represent the combined effects of surfactant concentration, mud contamination, relative shear rate, and contact time on the Cleaning Index. Interpolation for intermediate values is a straightforward process in the computer software. Clearly, these results are valid only for the surfactant and synthetic-based mud used in the supporting study.

Laboratory Tests for Well-Specific Displacements

The test matrix for the base laboratory study included as many combinations as was practical considering the available resources. This number of tests would make this prohibitive for routine applications.

Fortunately, the use of type curves and standard statistical analysis techniques helped to greatly reduce the testing requirements to a handful of tests. Furthermore, the statistical methods made it possible to characterize the sensitivity of four key variables (surfactant concentration, contamination level, velocity, and contact time) using a single index for each.

These improvements have considerably simplified implementation of the overall process. The use of well-specific laboratory tests and the sensitivity indexes are discussed further in later sections focusing on the software and case histories.

Interface Experiments and Modeling

Fluid-fluid interfaces created downhole while circulating can adversely impact displacements in several ways. Laboratory tests routinely check mud/spacer/brine compatibilities and access rheological consequences. However, other concerns include the lengths (volumes) of the various interfaces, their dynamic position in the wellbore, and contamination distributions created by the mixing energy.

Interface dynamics also is a critical issue in other displacement operations (cementing, for example) and has been heavily studied. Unfortunately, these processes are complex and not easily modeled. Computation fluid dynamics techniques would be overkill, especially when juxtaposed with the empirical mud-removal model. The alternative was to conduct special flow-loop testing to study displacement interfaces and develop suitable empirical models.

The fit-for-purpose flow loop shown in **Fig. 5** was constructed with 450 ft of 1.5-in (ID) pressure hose. A conductivity sensor was placed a short distance from the flow-loop inlet. Thereafter, sensors were added at 50, 100, 200 and 300 ft downstream along the hose length. For most tests, a high-conductivity brine pill was carefully inserted near the inlet of the flow loop completely filled with low-conductivity synthetic-based mud. Fluid densities and viscosities, flow rates, and spacer volumes were among the parameters that were varied to generate data for an empirical model.

Fig. 6 compares actual and theoretical $CaCl_2$ pill positions for a test run using 10-lb/gal synthetic-based mud at 18 gal/min flow rate. Pill volume was 2.5 gal. This technique tracked the start, end, and mixing of the pill during the test circulation. Steel coupons place at the end of the flow loop helped measure cleaning effectiveness.

Generalized sigmoid curves statistically manipulated to fit the data were used to define interface characteristics. Incorporation of the empirical model into the overall transient process and the effects of interfaces on mud-removal efficiency are discussed later in this paper.

Engineering Software

Basic software concepts presented earlier[1] were updated to address mud-removal and displacement interfaces. Wellbore and fluid elements were separated into two different calculation grids, based on how they behave during the displacement.

Static grids are composed of wellbore and tubular elements and are generated by subdividing the well into short depth segments, each with their own set of properties. Optimum segment lengths could be 50-100 ft, with allowances for discrete changes such as at casing points. A finite-difference technique can then be used for analysis. A detailed, but certainly not exhaustive list of static grid elements is provided in **Fig. 7a**; wellbore cleaning index and mud film thickness are among the properties associated with static grids. Static grids do not translate axially as fluids are pumped during displacement, but properties of each grid element are continuously adjusted as required for each time step.

Dynamic grids on the other hand are composed of elements that define fluid properties, and are translated past static grids during displacement. Dynamic grids typically are subdivided into 0.1 bbls increments, but different increments could also be used based on the application. Fluid type, surfactant concentration and mud contamination are among properties associated with dynamic grids as shown in **Fig. 7b**.

Either grid can be populated from different sources as well as interrelated calculations. For example, fluid locations can be directly calculated based on volumes pumped and spacer volumes. Mud-removal efficiency

however depends on calculations in previous time steps.

The traditional use of the software for volumes, pressure and hydraulics calculations have been discussed in more details elsewhere.[1] Continuous plots using the "rainbow chart" concept shows the position of each fluid involved in the displacement, and relevant flow rate and pressure curves. A computer-screen capture is shown in **Fig. 8**. The two multi-colored rainbow charts are synchronized vertically with volume pumped and horizontally with the well geometry. The upper pair applies to the work string while the lower pair shows the annulus. The rainbow chart also shows relevant pressure curves, such as pump pressures, bottomhole pressure, etc.

The software models the mud-removal process using transient interaction between dynamic and static grids. Removal efficiency depends on contact time, fluid velocity, surfactant type and concentration, and mud contamination, some of which are interrelated. Spacer contamination and removal efficiency are interrelated, each affecting the other. Higher efficiency results in more contamination since any mud removed gets incorporated into the spacer itself. Higher contamination on the other hand results in lower spacer effectiveness. The software continually adjusts effectiveness and contamination of the cleaning spacer as they travel through the wellbore during the displacement.

Fig. 9 shows a screen capture from the software at 420 bbls into the displacement. The left-most graphic displays the position of each fluid in the wellbore. The first plot on the left shows mud-removal efficiency, the second plot shows thickness of mud film, while the right-most plot shows mud contamination in each spacer. Only Spacer B was assumed to contain a chemical surfactant. As highlighted by the oval in **Fig. 9**, most of the mud-removal occurs in the leading part of Spacer B and it gets contaminated. Note that the tail-end of Spacer A also gets contaminated, but the leading-edge had little to no contamination.

Spacer contamination and concentration are also affected by fluid-fluid interfaces that develop during displacement. Laboratory studies indicate that interface mixing zone depend on, among many others, distance traveled, fluid velocity, and density and rheology difference between the two fluids. Empirical models based on laboratory data were developed and implemented in the software to calculate interface between two adjacent fluids. The software automatically adjusts surfactant concentration and contamination as the mixing zone continuously grows during the displacement. **Fig. 10** shows how the interface region between two adjacent fluids develops during displacement. The color bands show volumetric composition of each fluid in the mixed zone at any point in the displacement. The interface volume between spacers A and B was 25 bbls where indicated by the vertical line placed at 420 bbl. Some mud may have been removed by Spacer A due to solely hydrodynamic effects, however the majority of the mud-contamination was probably a result of mixing with the leading edge of mud-contaminated Spacer B.

The use of design overlays to evaluate various displacement design parameters has been published earlier.[1] **Fig. 11** shows a design overlay applied over **Fig. 8**. The selected design criterion was mud-removal efficiency greater than 90%. The cross-hatching indicates every position in the wellbore where more than 90% of the original mud-film was removed during the displacement. Note that only the riser section was not adequately clean perhaps due to insufficient annular velocity.

Interface mixing and mud contamination simulation results are presented in a flow-back graph as shown in **Fig. 12**. Similar to a flow-back test in the field using collected samples, the flow-back graph displays predicted return volumes, interface volumes and fluids compositions. Predicted spacer content is plotted as an "overlay" on ideal flow-back conditions. Note that the 3 spacers arrive at the surface before their theoretical arrival times. The spacers also continue to arrive beyond when they should have stopped coming out. Both are caused by mixing at the interfaces. The mud also continues to arrive with the spacers, beyond when it was expected to arrive. Mud removed from tubulars at any depth were incorporated into the fluid in contact with it, and hence arrived at the surface with the spacers.

Example Case History

A displacement spacer was required for a deepwater GoM well in which a 13.6-lb/gal synthetic drilling mud in the riser was to be indirectly displaced to seawater, followed by a direct displacement of the casing to 13.9-lb/gal $CaBr_2$ completion brine. Cleaning efficiency tests were performed to optimize the chemistry of the wash spacers for each displacement. The lab procedure as previously described was used, except the spacer testing for the riser was performed at 40°F. Several different surfactant solutions and surfactant/solvent combinations were tested. Table 3 and Figure 14 show the sensitivity ratings for each wash spacer tested. In general, the performance of the wash chemicals tested was most sensitive to velocity and contact time and was less affected by concentration in solution or by the amount of mud contamination. Of the solutions tested, surfactant A was the most sensitive to mud contamination, whereas solvent A was the most sensitive to flow rate. Figure 15 shows the modeling output for surfactant A, surfactant C and a combination of surfactant A and Solvent A.

Pump output and pipe diameters in the riser limited annular flow rates in the riser to about 120 ft/min. Based on the results of the lab testing and computer modeling,

a combination of surfactant A and solvent A was selected because of its capacity to hold whole mud and maintain cleaning efficiency. This system was circulated in the field with excellent results.

Conclusions

1. Mud-removal efficiency during mud-to-brine displacements can be effectively predicted by a transient process involving empirically derived engineering models.
2. Case histories demonstrate the successful use of this process in advanced software to design and evaluate displacement spacer trains with the ultimate goal of complete removal of residual mud from downhole tubulars in a single pass.
3. Results from simple laboratory tests used to determine wash-chemical effectiveness can be incorporated into the transient process using type curves based on generalized sigmoid relationships.
4. Empirical interfaces models based fit-for-purpose displacement flow loop studies reasonably match results from flow-back measurements.

Acknowledgments

The authors thank M-I SWACO for supporting this work and for permission to publish. They also thank personnel in the M-I SWACO Completion Fluids and Applied Engineering Laboratories for their valuable insights, suggestions, and assistance with the experimental studies.

Nomenclature

CI = *Cleaning Index*
e_1 = *exponent for* $t \leq \beta$
e_2 = *exponent for* $t \geq \beta$
m = *maximum Cleaning Index value (0.0 - 1.0)*
v = *level response curve (0.0 - 5.0)*
t = *normalized contact time*
β = *sigmoid curve crossover point*

References

1. Zamora, M., Sargent, T., and Froitland, T.: "Using Static 'Rainbow' Charts to Design Dynamic Completion-Fluid Displacements," AADE-02-DFWM-HO-10 presented at the 2002 AADE Technical Conference, Houston, 2-3 April 2002.
2. Foxenberg, W., *et al.*: "Validating the Quality of Mud-to-Brine Displacements," AADE-04-DF-HO-39 presented at the 2004 AADE Drilling Fluids Technical Conference, Houston, 6-7 April 2004.
3. Berg, E., Rakstang, O., and Sassen, A.: "An Efficient, Environmentally Acceptable, Clean Up System for Well Completions," *Oil-Gas European Magazine*, vol. 23, no. 3, pp. 12-16, 1977.
4. Davison, J.M., *et al.*: "Oil-Based Muds for Reservoir Drilling: Their Performance and Cleanup Characteristics," SPE 58798 presented at the 2000 SPE International Symposium on Formation Damage, Lafayette, LA, 23-24 Feb 2000.
5. Saasen, A., *et al.*: "Well Cleaning Performance," IADC/SPE 87204 presented at the 2004 IADC/SPE Drilling Conference, Dallas, TX, 2-4 March 2004.
6. Berry, S.L.: "Optimization of Synthetic-Based and Oil-Based Mud Displacements with an Emulsion-Based Displacement Spacer System," SPE 95273 presented at the 2005 SPE Annual Technical Conference and Exhibition, Dallas, TX, 9-12 Oct 2005.

Speed	Surf%	Cont%	0.5m	1.5m	3.7m	5.0m	10m
0.9	5	75					
6	5	75					
60	5	75					
100	5	75					
300	5	75	0.50	0.50	0.50	0.50	0.50
600	5	75					
0.9	5	50					
6	5	50	0.00	0.00	0.00	0.25	
60	5	50	0.00	0.25	0.25	0.50	
100	5	50	0.00	0.25	0.50	0.50	
300	5	50					
600	5	50	1.00	1.00	1.00	1.00	1.00
0.9	5	25					
6	5	25	0.00	0.00	0.00	0.25	
60	5	25	0.00	0.25	0.25	0.50	
100	5	25	0.00	0.25	0.50	0.50	
300	5	25					
600	5	25	1.00	1.00	1.00	1.00	1.00
0.9	5	0					
6	5	0	0.00	0.00	0.00	0.25	
60	5	0	0.00	0.25	0.50	0.75	
100	5	0	0.00	0.25	0.50	0.75	
300	5	0					
600	5	0	1.00	1.00	1.00	1.00	1.00

Table 1 – Sample laboratory XClean data.

Speed	Surf %	Cont %	Max	Level
0.9	5	75	0.02	1.8
6	5	75	0.05	2.0
60	5	75	0.22	2.6
100	5	75	0.30	3.0
300	5	75	0.50	4.3
600	5	75	0.75	5.0
0.9	5	50	0.13	1.8
6	5	50	0.17	2.0
60	5	50	0.35	2.6
100	5	50	0.44	3.0
300	5	50	0.65	4.3
600	5	50	0.90	5.0
0.9	5	25	0.18	1.8
6	5	25	0.22	2.0
60	5	25	0.46	2.6
100	5	25	0.55	3.0
300	5	25	0.80	4.3
600	5	25	0.95	5.0
0.9	5	0	0.27	1.8
6	5	0	0.35	2.0
60	5	0	0.70	2.6
100	5	0	0.80	3.0
300	5	0	0.96	4.3
600	5	0	1.00	5.0

Table 2 – Sample XClean data showing original (black) and synthesized (blue) data.

Riser	Wash Chemical Concentration	Velocity	Contact Time	SBM Contamination
Surf A	4.9	2.16	1.93	2.37
Surf B	4.6	3.22	1	4.45
Surf C	4.79	1.9	2.49	4.66
Solv A	4.56	1.09	1.17	3.63
Solv B	3.63	1.29	2.22	4.95
50:50 Surf A:Solv A	3.99	2.56	1.56	1.64
50:50 Surf C:Solv B	4.41	2.45	4.12	3.51

Table 3 - Sensitivity variables for 13.6-lb/gal SBM and various wash chemicals

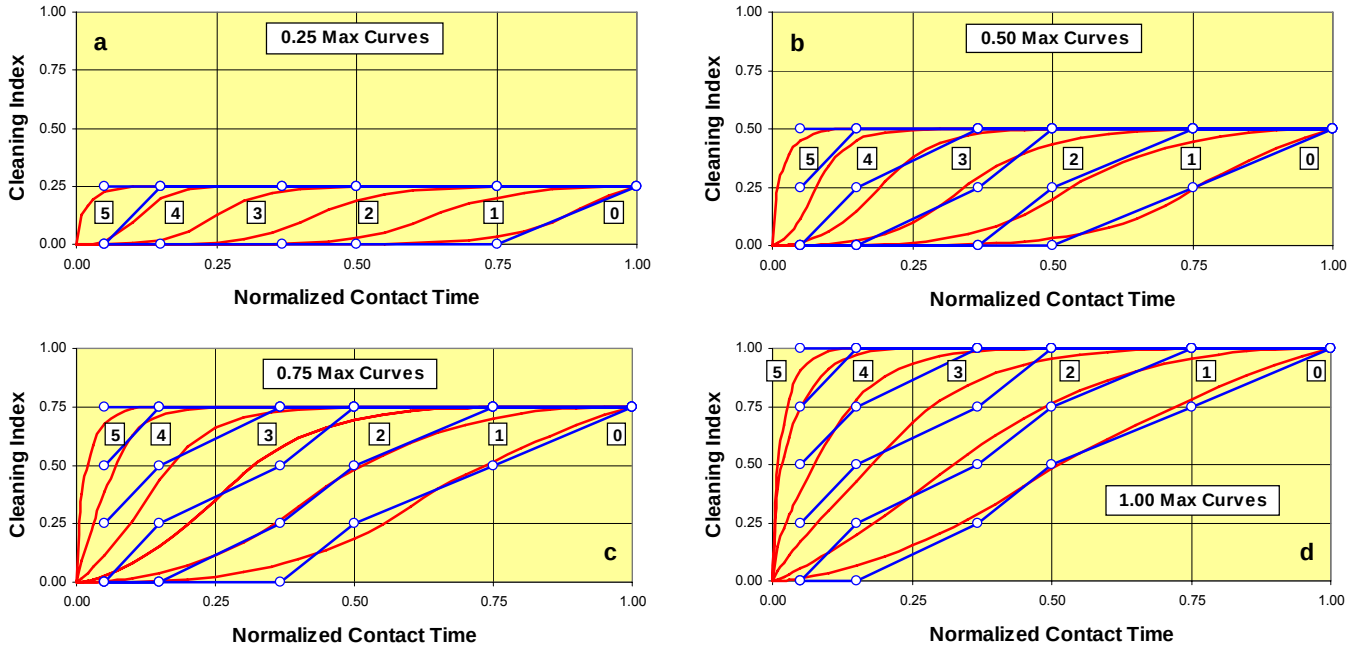

Fig. 1 - Cleaning index as a function of normalized contact time for discrete "Max" values.

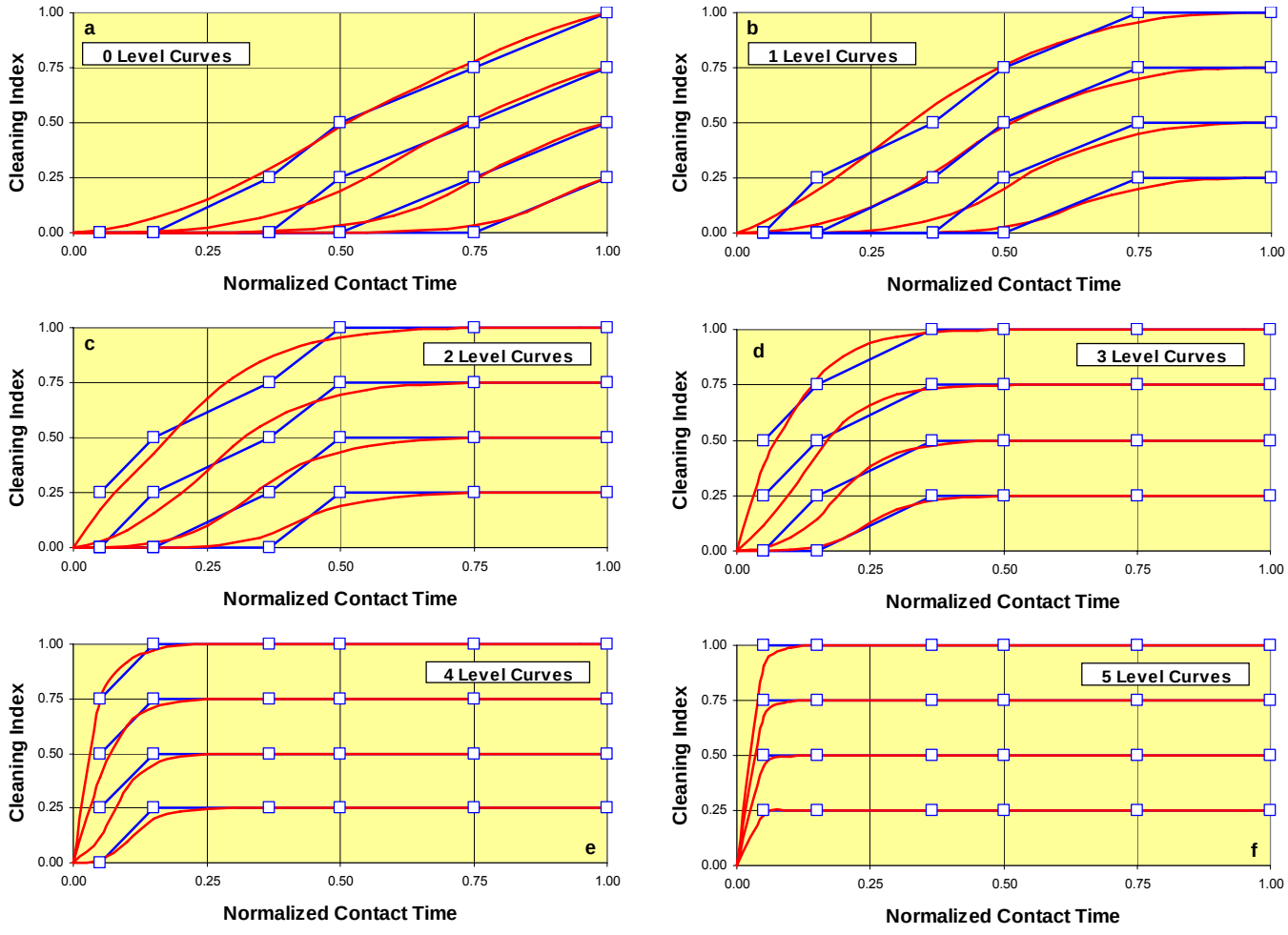

Fig. 2 - Cleaning index as a function of normalized contact time for discrete "Level" values.

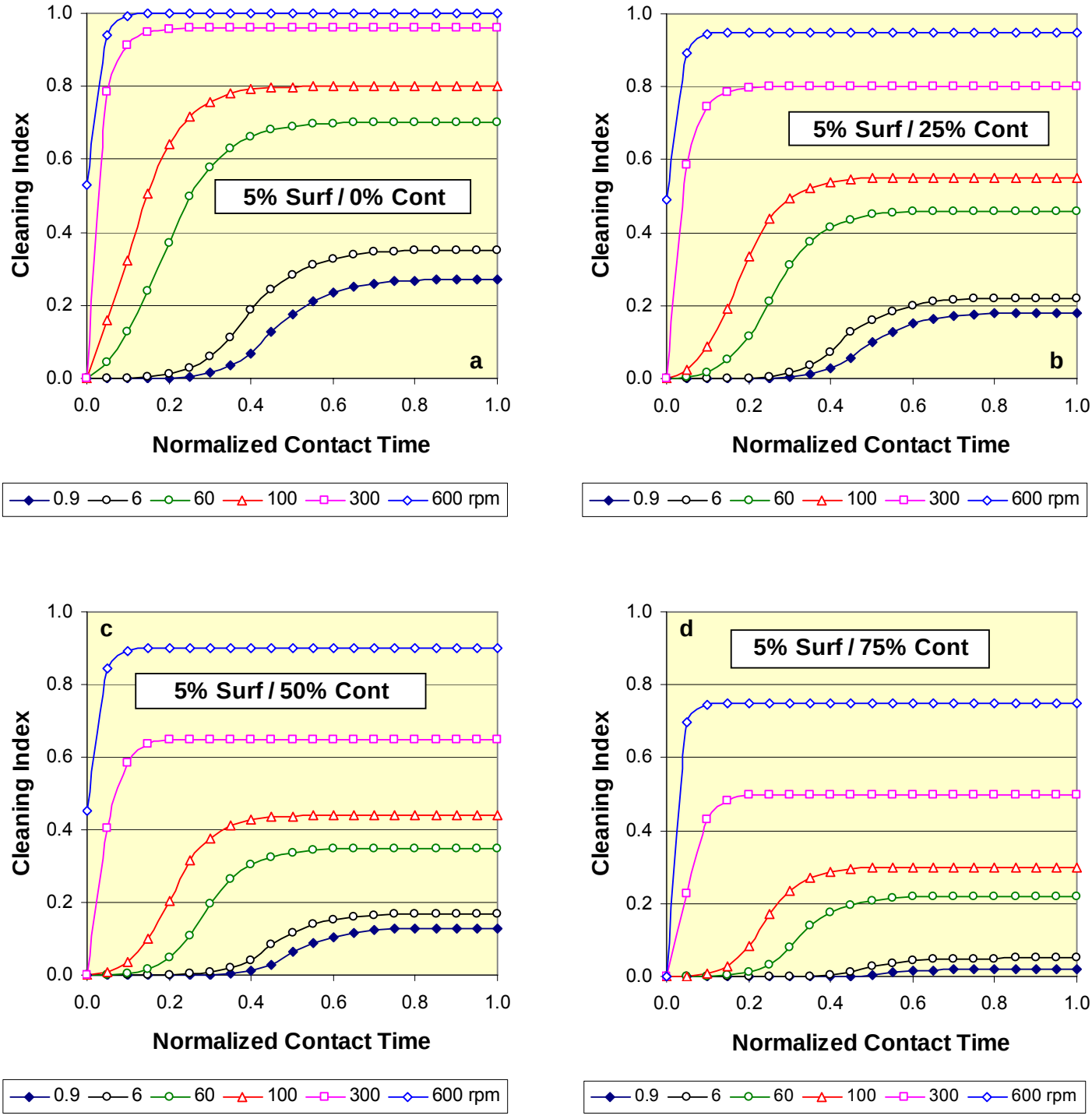

Fig. 3 - Sample results showing contamination effect on cleaning index with 5% surfactant solution.

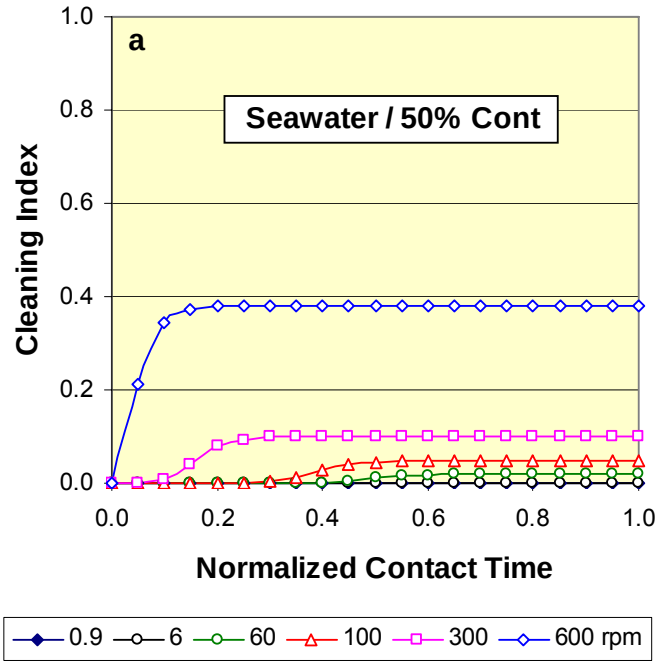

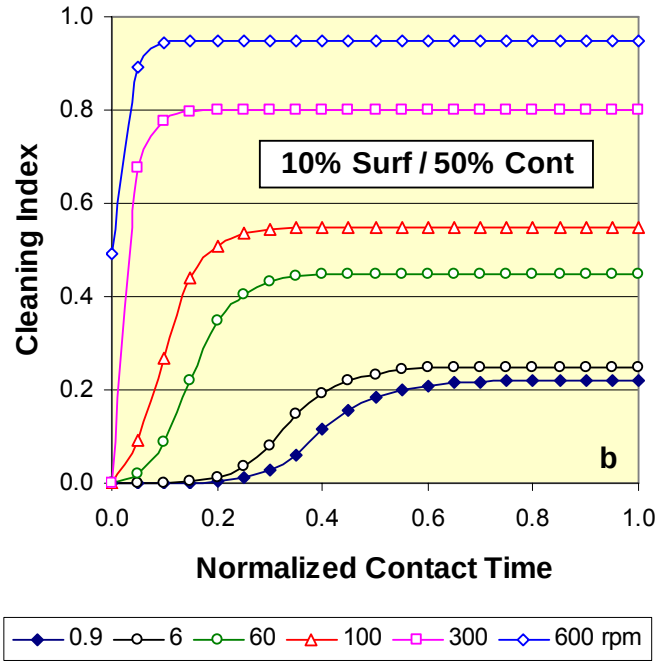

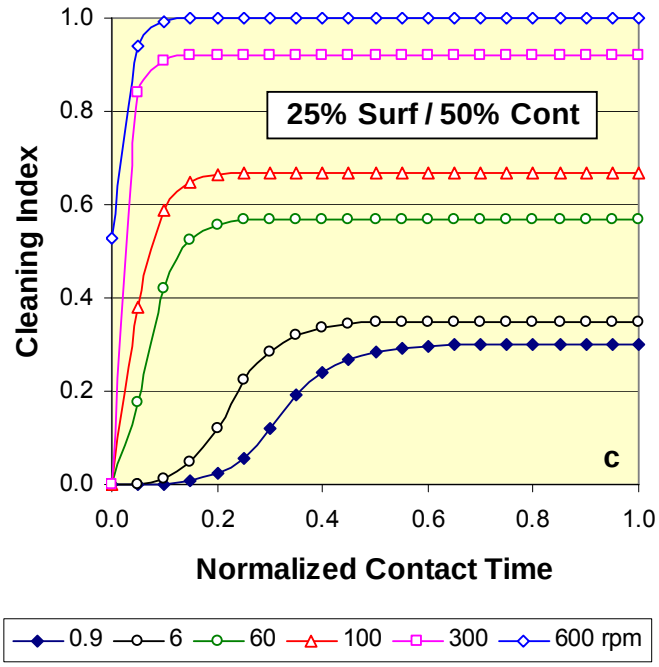

Fig. 4 - Sample results showing effect of surfactant concentration cleaning index with 50% contamination.

Fig. 5 - Flow loop used for displacement interfaces study.

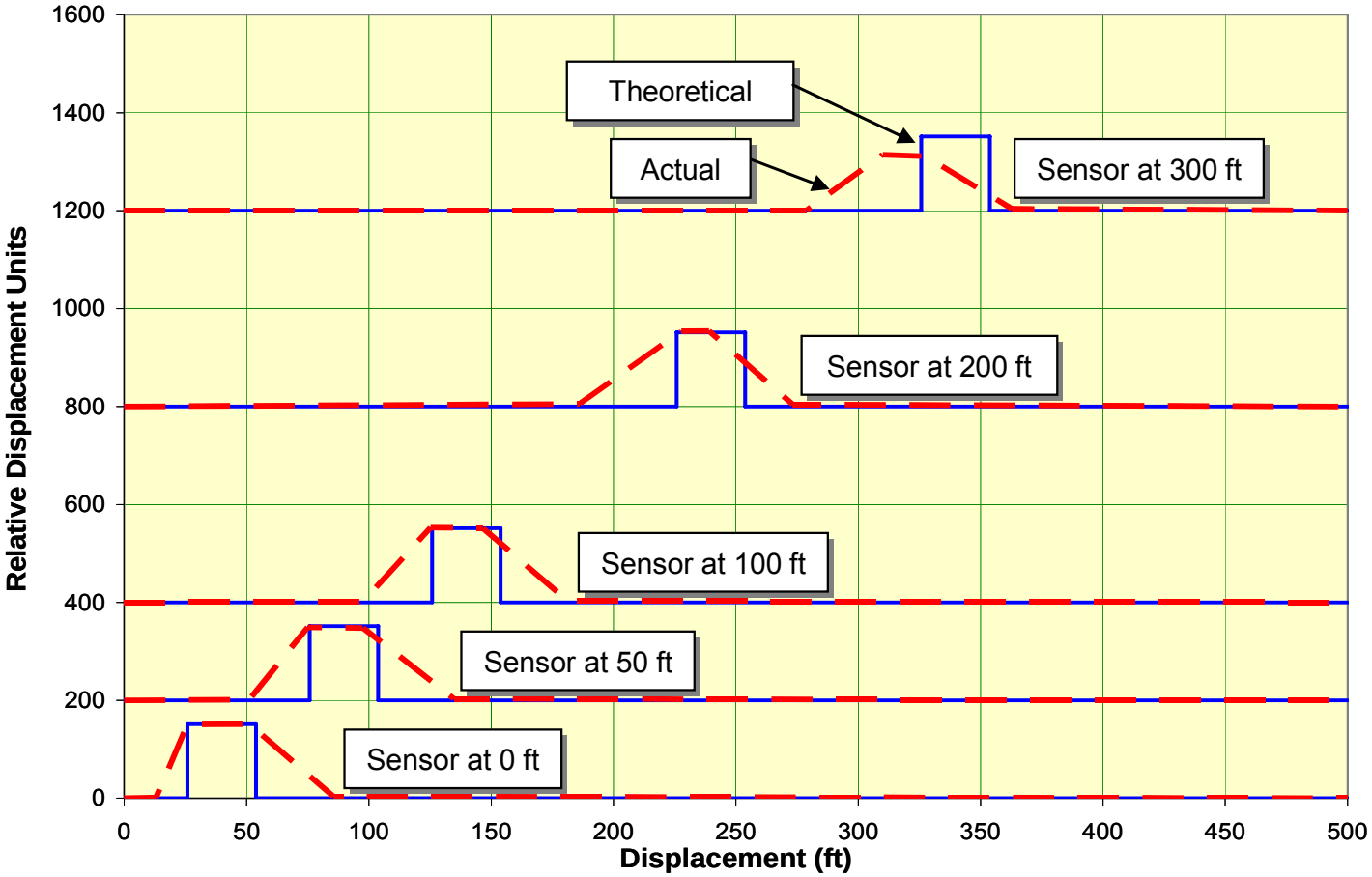

Fig. 6 – Displacement interfaces results showing theoretical and actual positions of a $CaCl_2$ pill displacing a 10-lb/gal synthetic-based mud.

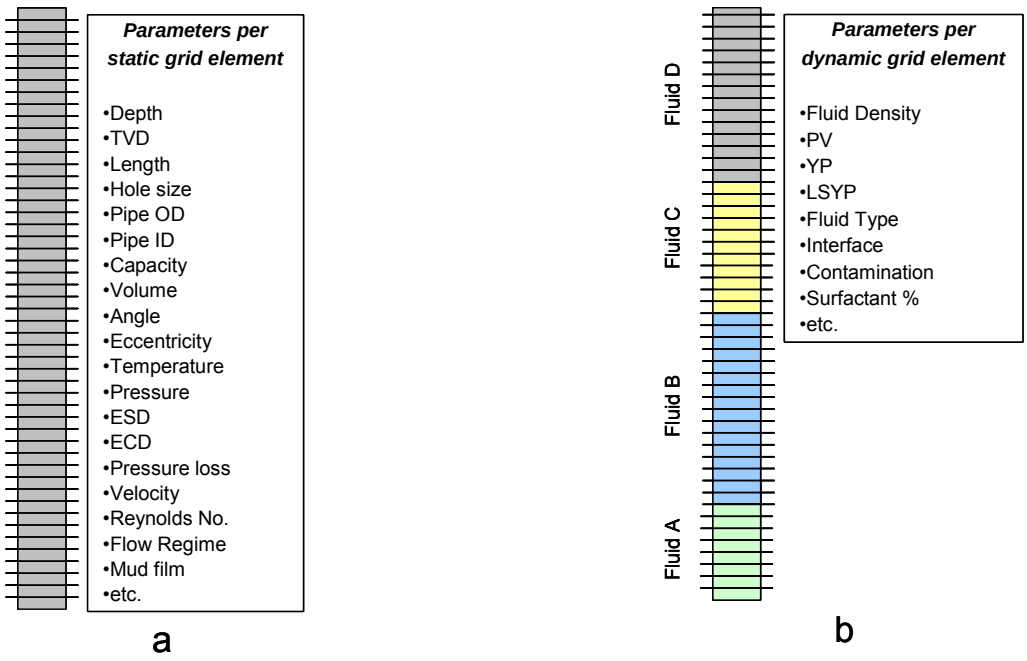

Fig. 7 – Parameters defined for static (a) and dynamic (b) grids.

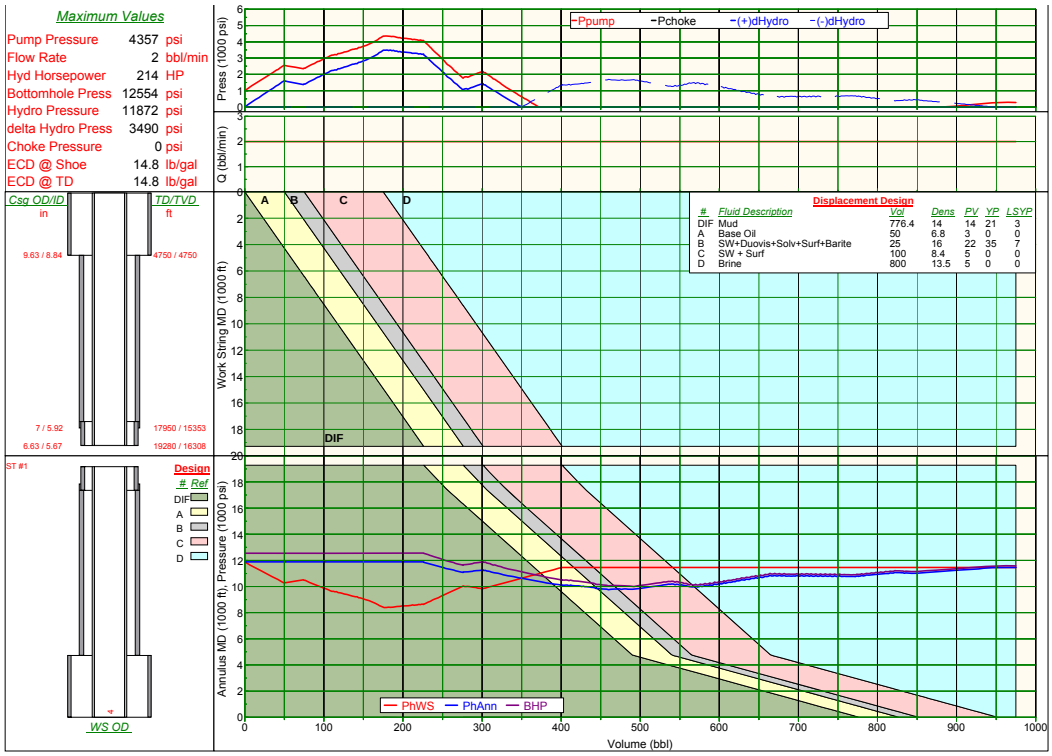

Fig. 8 - Sample Rainbow chart showing fluid positions and pressures during displacement.

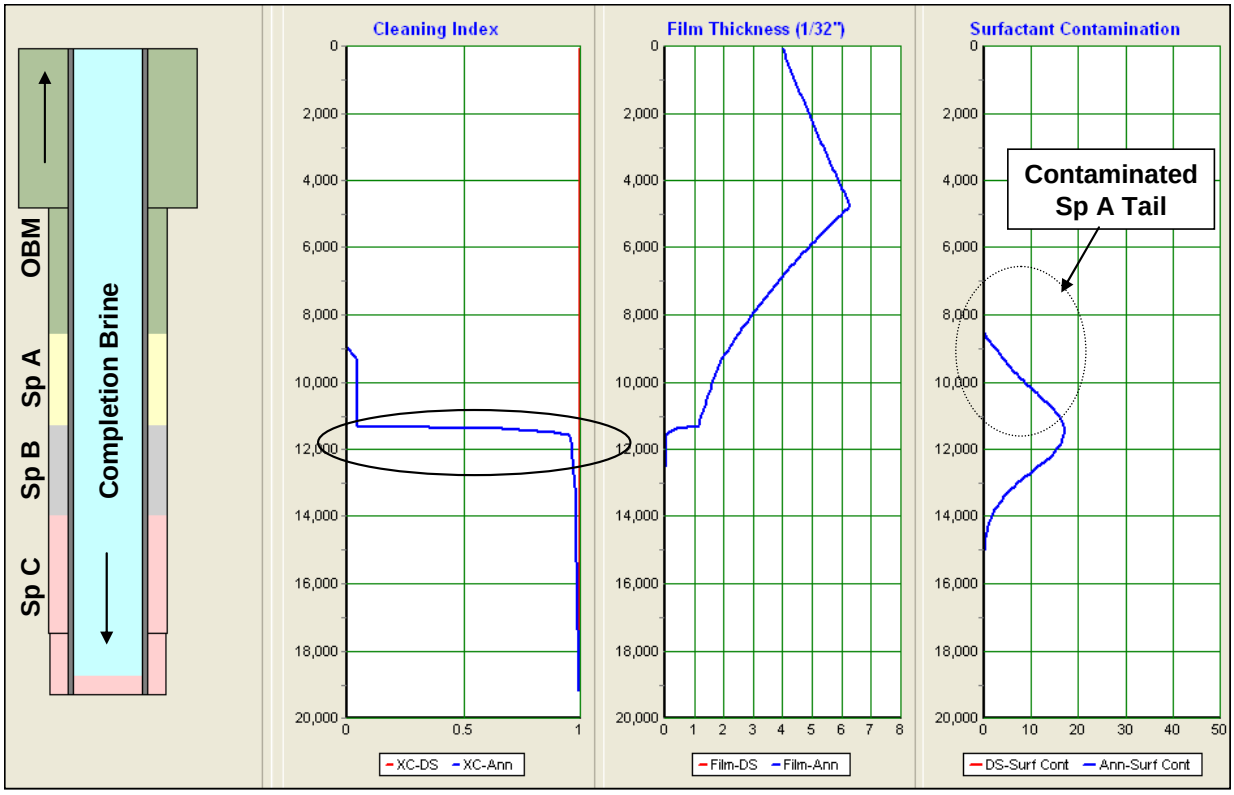

Fig. 9 – Screen capture showing wellbore cleaning profiles at 420 bbl into the displacement.

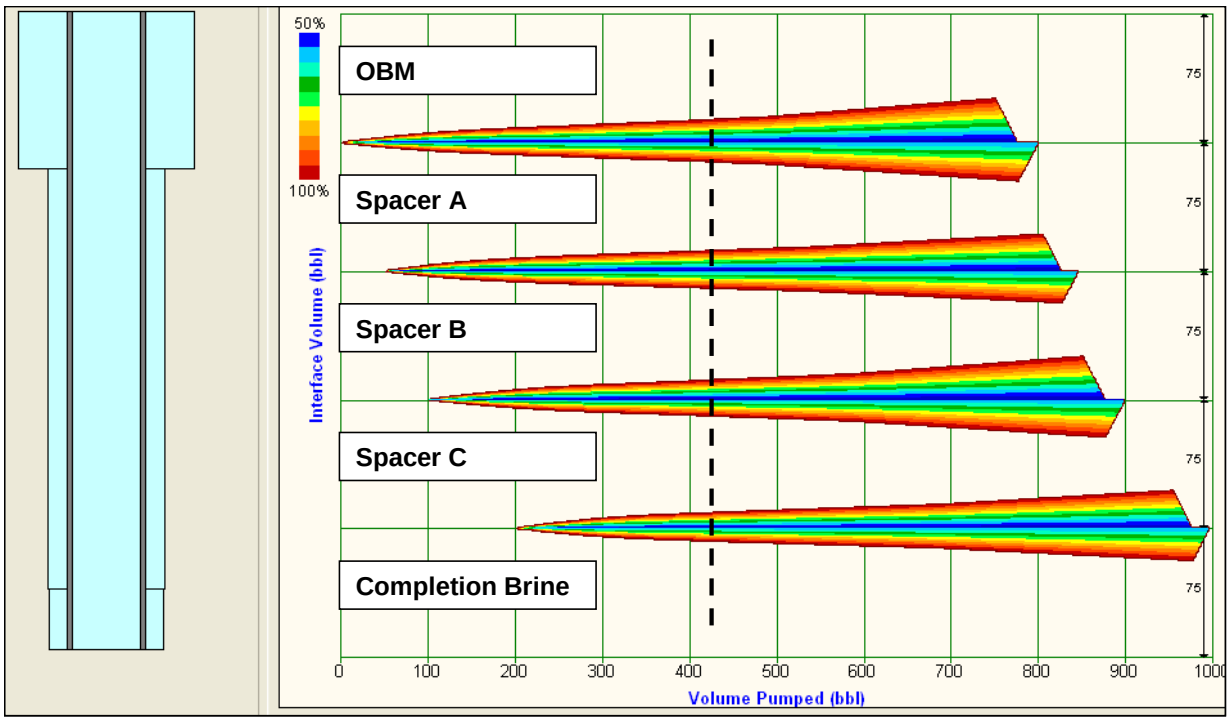

Fig. 10 - Interface volumes and composition between adjacent fluids during displacement. Note interface volume between spacers A and B is 25 bbl where indicated with the vertical line. The color bands indicate fluid distribution in the interface region; blue indicates 50% of each fluid while red indicates 100% of fluid on either end of interface.

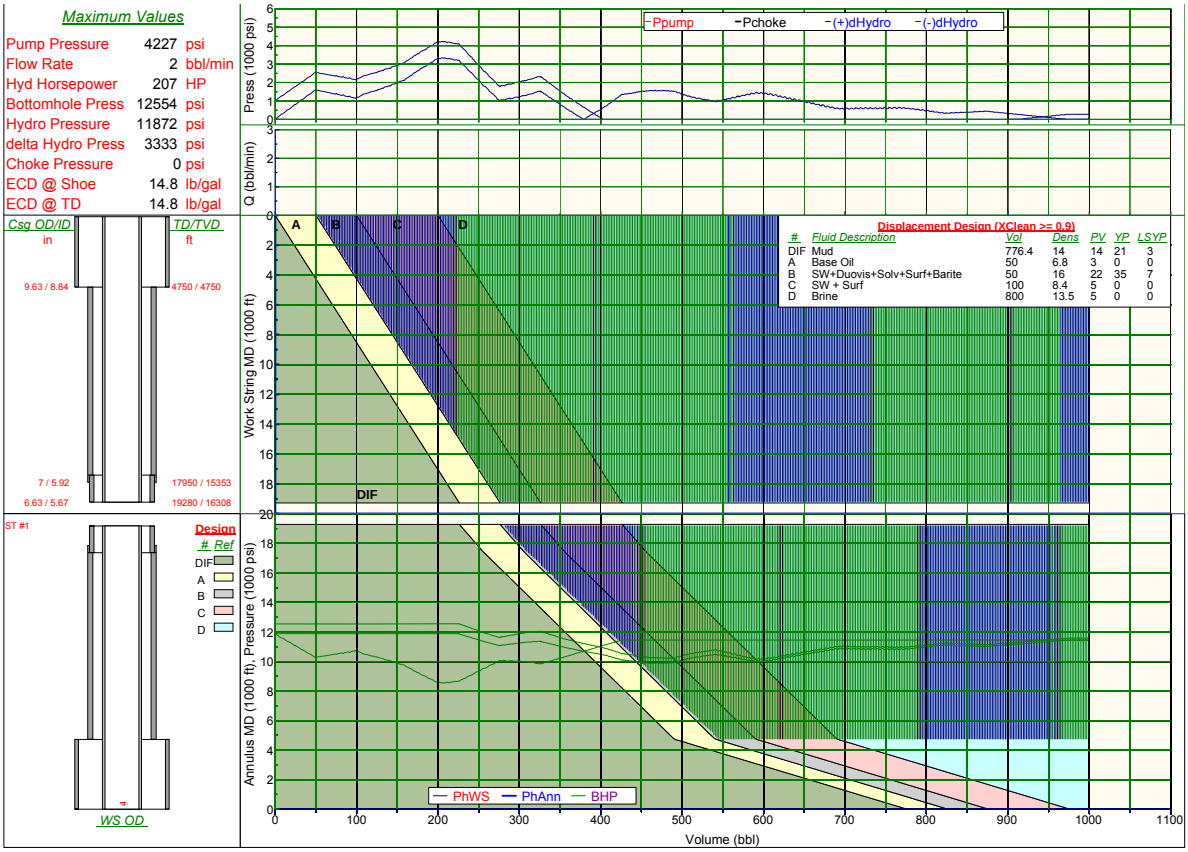

Fig. 11 - Design overlay applied to **Fig. 8**. Cross-hatched area indicates mud-removal efficiencies greater than 90%. The arrow points to the riser section with insufficient removal efficiency.

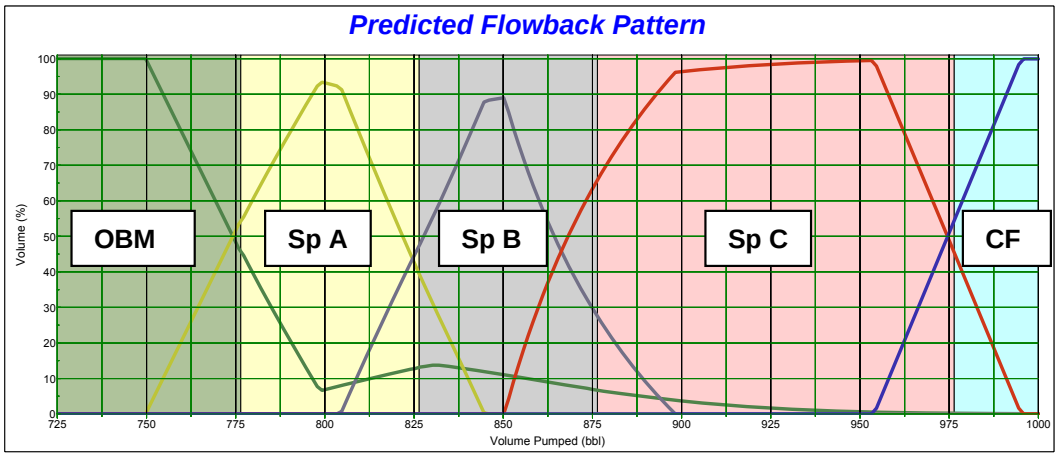

Fig. 12 - Predicted flowback pattern. The shaded portions represent "ideal" flowback conditions. Note spacers are detected earlier than expected. Also note mud continues to arrive almost 200 bbls after it should have left the wellbore.

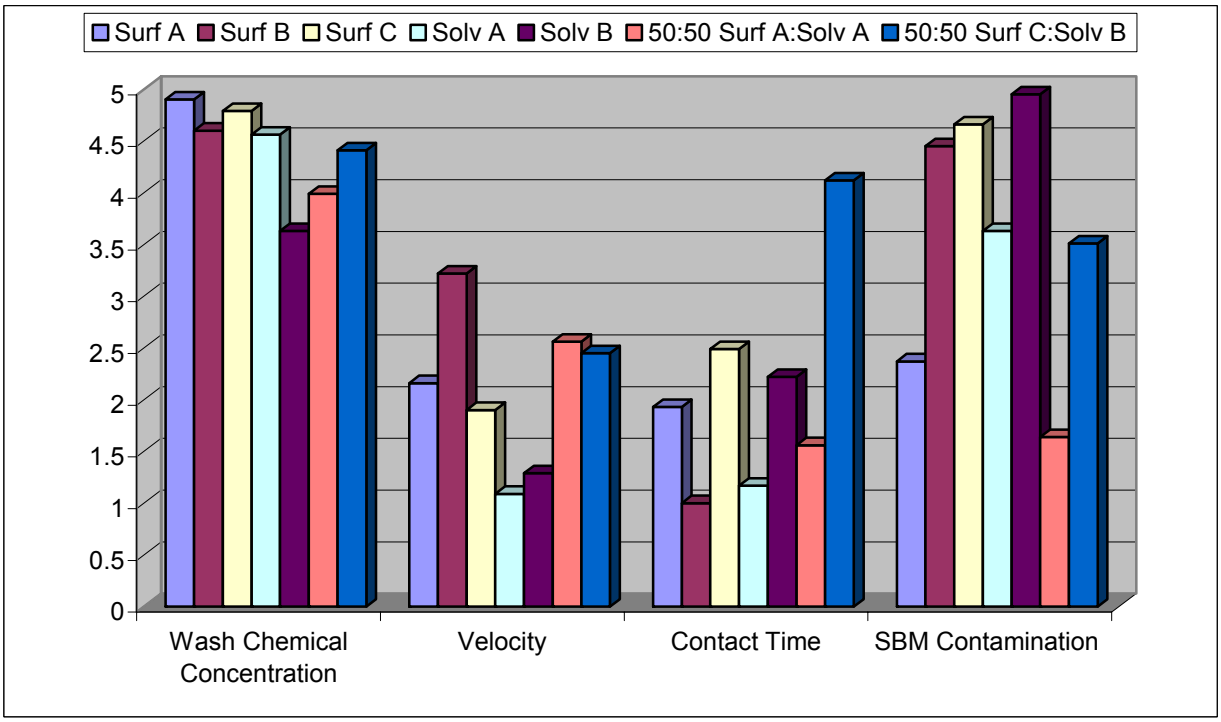

Fig. 13 – Graphical representation of sensitivity variables for various wash chemicals tested for riser example.

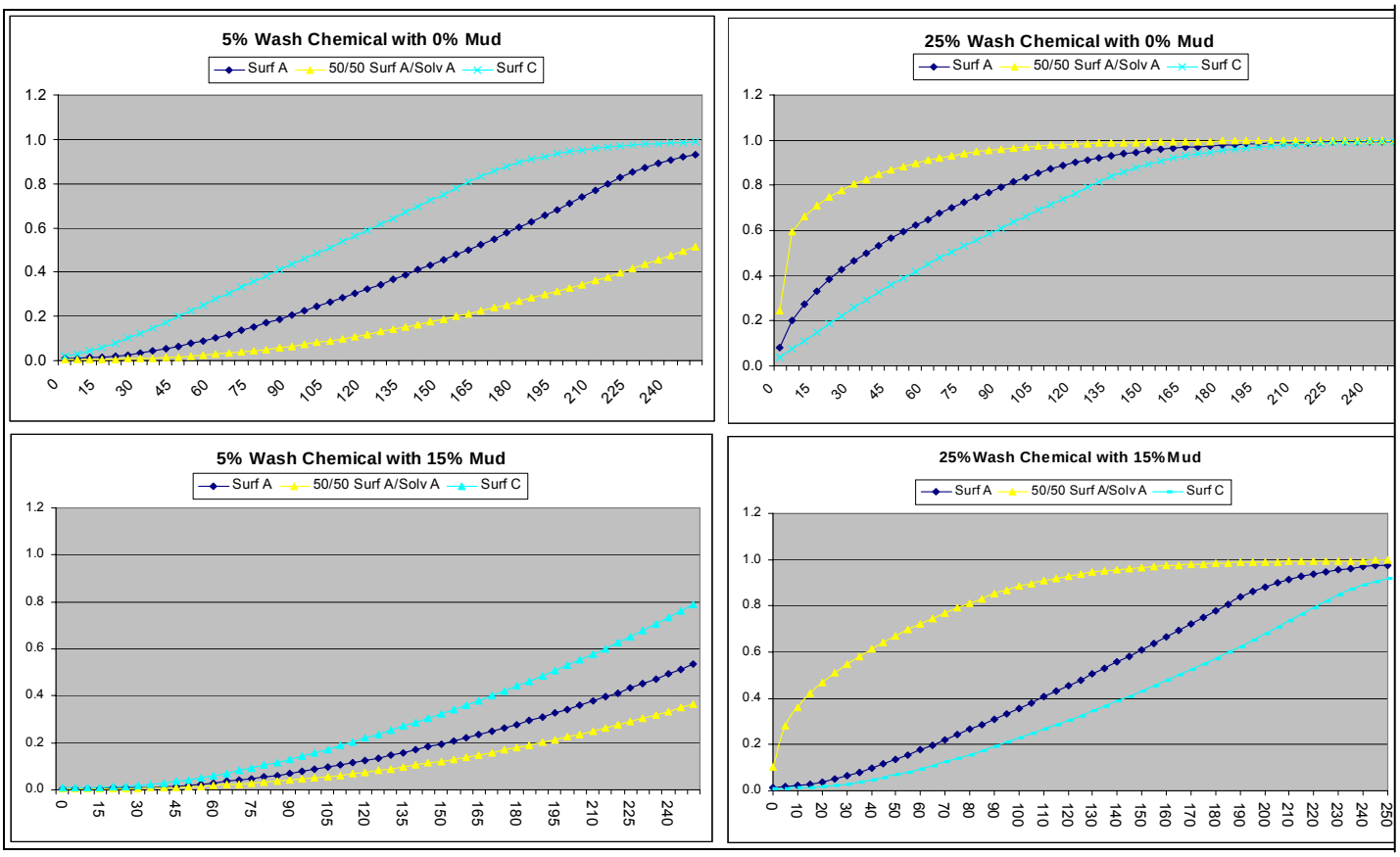

Figure 14 – Simulation of wash chemical efficiency tests for riser displacement.